





REPORT

microRNAs selectively protect hub cells of the germline stem cell niche from apoptosis

Marina Volin , Maayan Zohar-Fux , Oren Gonen, Lilach Porat-Kuperstein , and Hila Toledano 

Genotoxic stress such as irradiation causes a temporary halt in tissue regeneration. The ability to regain regeneration depends on the type of cells that survived the assault. Previous studies showed that this propensity is usually held by the tissue-specific stem cells. However, stem cells cannot maintain their unique properties without the support of their surrounding niche cells. In this study, we show that exposure of *Drosophila melanogaster* to extremely high levels of irradiation temporarily arrests spermatogenesis and kills half of the stem cells. In marked contrast, the hub cells that constitute a major component of the niche remain completely intact. We further show that this atypical resistance to cell death relies on the expression of certain antiapoptotic microRNAs (miRNAs) that are selectively expressed in the hub and keep the cells inert to apoptotic stress signals. We propose that at the tissue level, protection of a specific group of niche cells from apoptosis underlies ongoing stem cell turnover and tissue regeneration.

Introduction

Cells in a given tissue can respond differently to stress signals based on their balance between prosurvival and death-promoting factors (Bree et al., 2002). Homeostasis and repair of regenerative tissues such as hair, skin, and testis is often severely impeded by stress signals (e.g., irradiation) but can also regain function once the stress has been removed. Tissue regeneration is controlled by rare populations of residential adult stem cells that often reside in direct contact with microenvironment niche cells (Lin, 2002; Jones and Wagers, 2008). The regenerative potential of adult stem cells relies on their capability to yield two types of cells upon division: one that detaches from the niche, differentiates, and replaces lost cells within the tissue, and one that is kept within the niche as a stem cell for future use (Morrison and Spradling, 2008). Therefore, the niche serves as a control unit that regulates the rate of stem cell proliferation and protects the overall stem cell pool from depletion.

In this study, we used the model system of *Drosophila melanogaster* testis to identify the exact cells within a regenerative tissue that are most resistant to apoptotic signals and reveal the core that enables tissue recovery. Spermatogenesis is governed by germline stem cells (GSCs) that share the niche together with cyst stem cells (CySCs) and adhere around a sphere of somatic cells called the hub (Fig. 1 A). The hub is a compact cluster of ~12 cells that secrete short-range signals and express adhesion molecules to maintain the surrounding stem cells (Kiger et al., 2001; Tulina and Matunis, 2001; Leatherman and Dinardo, 2010). One of the

two daughter cells that are formed by a GSC division remains adherent to the hub for self-renewal, while the other is displaced and undergoes transit amplification divisions before becoming a terminally differentiated spermatocyte (Insko et al., 2009).

GSCs in male and female gonads as well as intestinal stem cells were shown to be more resistant to cell death compared with their differentiated progeny (Xing et al., 2015). However, because the niche is critical in maintaining the stem cells in their undifferentiated state, we postulated that the hub cells use an even more stringent mechanism to resist genotoxic signals. We also proposed that the protection of the niche from demise involves specific genetic programming that is tightly regulated by miRNAs. miRNAs are an established class of posttranscriptional RNA regulators that negatively regulate gene expression through translational inhibition and/or degradation of mRNA targets (Djuranovic et al., 2012). miRNAs identify their targets through base-pairing of six to eight seed elements with recognition sites located mainly in the 3' UTR or within the ORF of the mRNA (Brodersen and Voinnet, 2009). All miRNAs are encoded in the genome itself, and their final processing into functional units occurs in the cytoplasm by a single enzyme, Dicer1 (Dcr1; Ghildiyal and Zamore, 2009; Saxe and Lin, 2011). Antiapoptotic miRNAs such as *bantam* were previously shown to promote tissue growth and prevent apoptosis during development (Brennecke et al., 2003; Ge et al., 2012). In this study, we show that the postmitotic hub cells are highly resistant to apoptosis

Department of Human Biology, Faculty of Natural Sciences, University of Haifa, Haifa, Israel.

Correspondence to Hila Toledano: hila@sci.haifa.ac.il.

© 2018 Volin et al. This article is distributed under the terms of an Attribution–Noncommercial–Share Alike–No Mirror Sites license for the first six months after the publication date (see <http://www.rupress.org/terms/>). After six months it is available under a Creative Commons License (Attribution–Noncommercial–Share Alike 4.0 International license, as described at <https://creativecommons.org/licenses/by-nc-sa/4.0/>).

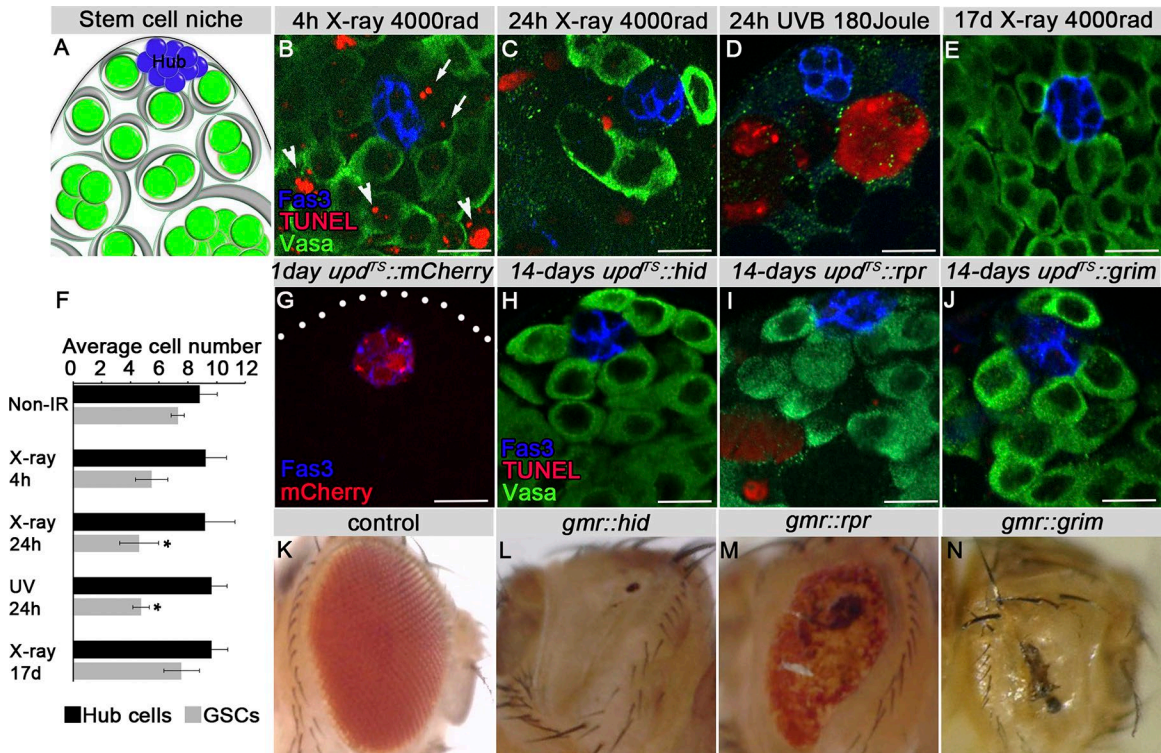


Figure 1. The inability of x-ray, UV, and proapoptotic genes to induce hub cell death. (A) Side view schematic representation of the GSC niche. Hub cells (blue), cyst cells (gray), GSCs, and spermatogonia (green). (B–E) Testes of WT flies that were immunostained for Fas3 (hub; blue), Vasa (germ cells; green), and TUNEL (red) at the indicated time after x-ray (B, $n = 45$; C, $n = 30$, 4,000 rads) and UVB exposure (D, $n = 37$, $180 \text{ kg} \cdot \text{m}^{-2} \cdot \text{s}^{-2}$). Arrows and arrowheads mark TUNEL-positive GSCs and spermatogonia, respectively. Note that tissue regeneration occurs 17 d after x-ray exposure (E, $n = 26$). (F) Shown are average number per testis of GSCs (gray) and hub cells (black) after irradiation along with 95% confidence intervals (error bars). Note that GSC average number decreases 24 h after irradiation and increases after 17 d, whereas hub cell number is not affected. Statistical significance was determined by one-way ANOVA, and post hoc analysis was performed with Tukey multicomparison test. *, $P \leq 0.05$ GSC average number between 24 h x-ray/UV irradiated and nonirradiated. (G) mCherry overexpression (*upd^{TS}::mCherry*) is induced only in the hub after 1 d at the restrictive temperature (29°C), Fas3 (hub; blue), and mCherry (red). Dashed line marks the apical edge of the testis. (H–J) Overexpression of *hid* (H, *upd^{TS}::hid*, $n = 39$), *rpr* (I, *upd^{TS}::rpr*, $n = 97$), or *grim* (J, *upd^{TS}::grim*, $n = 60$) in the hub for 14 d at 29°C did not result in hub cell death. Fas3 (hub; blue), Vasa (germ cells; green), and TUNEL (red). (K) Eye of control (*gmr::GAL4* outcrossed to *w¹¹¹⁸*). (L–N) Overexpression of *hid* (L, *gmr::hid*), *rpr* (M, *gmr::rpr*), or *grim* (N, *gmr::grim*) induces eye cell death. All images in all figures are single sections; scale bars are $10 \mu\text{m}$.

induction. To identify the mRNAs and miRNAs that protect the niche from apoptosis, we used transcriptomics and miRNAomics, which revealed the identity of several miRNAs that antagonize apoptosis and create a durable niche that enables spermatogenesis under harmful conditions.

Results and discussion

Hub cells are resistant to cell death

To identify the cells that are most resistant to apoptosis within the regenerative *Drosophila* testis, we exposed young adult flies to high doses of damage-induced UVB ($180 \text{ kg} \cdot \text{m}^{-2} \cdot \text{s}^{-2}$) or x-ray irradiation (4,000 rads). We examined testes after irradiation at multiple time points with TUNEL to in situ label DNA fragments characteristic of apoptotic cells (Arama and Steller, 2006). TUNEL staining 4 h after irradiation showed that although GSCs and spermatogonia germ cells underwent massive apoptosis, the hub cells were completely intact and did not show any detectable TUNEL signal (Fig. 1, A, B, and F). 24 h after irradiation, most spermatogonia germ cells as well as 40% of GSCs disappeared, while there was no change in the number of the hub cells (Fig. 1, C, D, and F). After 17 d of recovery after irradiation, the whole niche re-

generated, and spermatogenesis was completely regained (Fig. 1, E and F). These results suggest that the hub cells use a unique resistance mechanism against damage-induced irradiation that nonautonomously enables recovery of spermatogenesis.

To challenge the hub resistance, we used the temporal and regional gene expression targeting (TARGET) system to induce strong apoptosis activators only in the hub of the entire testis (McGuire et al., 2004). Activation of inhibitor of apoptosis protein (IAP) antagonists *head involution defective* (*hid*), *reaper* (*rpr*), and/or *grim* is the final point of no return in the induction of apoptosis (Steller, 2008; Xu et al., 2009). Studies show that in their absence, apoptosis is completely blocked, while their ectopic expression confers massive apoptosis (Grether et al., 1995; Chen et al., 1996). To avoid apoptosis induction during development, TARGET flies were raised at a permissive temperature of 18°C until eclosion, and 1-d-old adult males were then moved to the restrictive temperature of 29°C to induce ectopic expression of IAP antagonists in the hub. To confirm that our TARGET system (*upd-GAL4; GAL80^{TS}*) indeed drives expression at 29°C only in the hub of the testis, we ectopically expressed *UAS-mCherry* and detected a strong, hub-specific mCherry signal after 24 h (Figs. 1 G and S1 A). Strikingly, overexpression of *hid*, *rpr*, or *grim* transgenes in

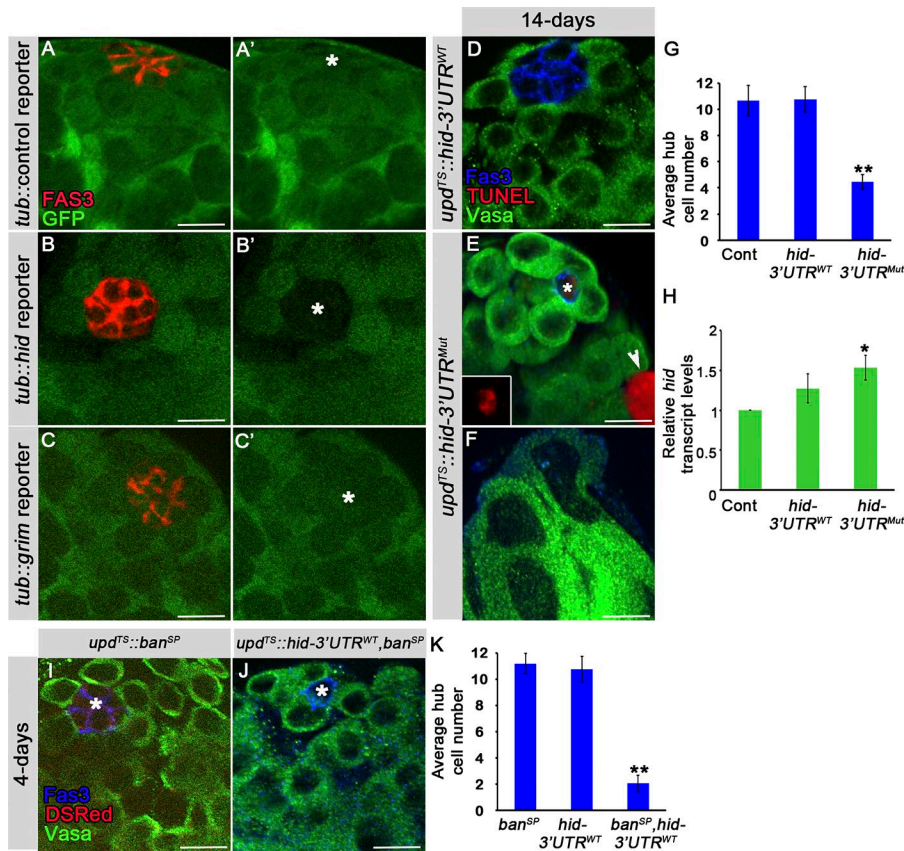


Figure 2. miRNAs in the stem cell niche prevent hub cell death. (A–C') Apical tip of control, *hid*, or *grim* GFP reporters (green) expressed under Tubulin promoter and immunostained for Fas3 (red and asterisks; hub). Control GFP reporter (A and A'), *hid* 3' UTR GFP reporter (B and B'), and *grim* 3' UTR GFP reporter (C and C'). Note reduced GFP expression in the hub. (D–G) Testes of flies raised for 14 d at 29°C immunostained for Fas3 (hub; blue), TUNEL (red and inset), and Vasa (germ cells; green). (D) Overexpression of *hid-3'UTR^{WT}* in the hub (*upd^{TS}::hid-3'UTR^{WT}*). (E and F) Overexpression in the hub of *hid* carrying two point mutations in *bantam* recognition sites (*upd^{TS}::hid-3'UTR^{Mut}*) results in hub (asterisk) cell death (E) or complete niche loss (F). Arrowhead marks spontaneous GCD and serves as TUNEL control. (G) Shown are average number of hub cells per testis along with 95% confidence intervals (error bars). Total number of testes scored: control (*upd-GAL4;GAL80^{TS}* outcrossed to *w¹¹¹⁸*), *n* = 29; *upd^{TS}::hid-3'UTR^{WT}*, *n* = 39; and *upd^{TS}::hid-3'UTR^{Mut}*, *n* = 55. Statistical significance was determined as in Fig. 1 F; **, *P* ≤ 0.005 between *hid-3'UTR^{Mut}* and both *hid-3'UTR^{WT}* and control. (H) qRT-PCR of *hid* transcript levels relative to *rpl32* of RNA extracted from testes of control or *hid-3'UTR^{WT}* or *hid-3'UTR^{Mut}*; levels are normalized to control. Error bars denote SD of three biological repeats each in triplicate measurements. *, *P* < 0.05 between *hid-3'UTR^{Mut}* and control. (I–K) Overexpression of *hid-3'UTR^{WT}* together with *bantam* sponge for 4 d at 29°C resulted in hub cell loss. (K) Shown are average number of hub cells per testis along with 95% confidence intervals (error bars). The total number of testes scored: *upd^{TS}::ban^{SP}*, *n* = 38; *upd^{TS}::hid-3'UTR^{WT}*, *n* = 37; and *upd^{TS}::hid-3'UTR^{WT}, ban^{SP}*, *n* = 42. Statistical significance was determined as in Fig. 1 F; **, *P* ≤ 0.005 between *hid-3'UTR^{WT}*, *ban^{SP}* and both *ban^{SP}* and *hid-3'UTR^{WT}*.

the hub of adult males for 14 d at the restrictive temperature was unable to induce cell death (Fig. 1, H–J). A subsequent quantitative RT-PCR (qRT-PCR) analysis verified that these overexpressed transgenes are indeed transcribed in the hub (Fig. S1 B). To ascertain that our transgenes are able to cause apoptosis elsewhere, we ectopically expressed them by two alternative approaches: using the same driver during development (*upd-GAL4*) and in the *Drosophila* eye (*gmr-GAL4*). As expected, overexpression of these genes caused larvae lethality (not depicted) and eye loss (Fig. 1, K–N), respectively. Together, these data suggest that although the *hid*, *rpr*, and *grim* transgenes have the potential to confer apoptosis, their ability to do so in the hub is markedly attenuated.

miRNAs in the hub antagonize apoptosis

To find whether there are factors within the hub that antagonize the overexpression of *hid* and *grim* via sequences located in their 3' UTR, we examined the expression pattern of GFP reporters that are attached to the 3' UTR of either *hid* or *grim* (Brennecke et al., 2003). As depicted in Fig. 2 (A–C) compared with the control GFP reporter that expresses uniformly in the hub and germ cells, the presence of *hid* or *grim* 3' UTRs silenced GFP expression

in the hub. These results suggest that miRNAs and/or other factors that inhibit translation via the 3' UTRs of *hid* and *grim* are expressed in the hub.

The 3' UTR of *hid* can be regulated by >20 miRNAs and includes five recognition sites for the *bantam* miRNA. Because *bantam* was previously shown to down-regulate the expression of *hid* (Brennecke et al., 2003), we tested whether *hid*-induced apoptosis is blocked by *bantam* in the hub. First, we attempted to generate UAS transgenic lines with insertion of four and five point mutations in the *bantam* recognition sites. However, despite our best efforts, these mutations were lethal and no transgenic flies were obtained, indicating that the leakiness of expression manifested by these constructs was sufficient to induce apoptosis. Therefore, we ectopically induced the expression of *hid-3'UTR^{Mut}* (*upd-GAL4;UAS-hid-3'UTR^{Mut},GAL80^{TS}*) that carries two point mutations at the *bantam* recognition sites and compared it with the transgene that contains the WT *hid* 3' UTR (*upd-GAL4;UAS-hid-3'UTR^{WT},GAL80^{TS}*). After 14 d at the restrictive temperature (29°C), the average hub cell number of *hid-3'UTR^{Mut}* was reduced by 80%, and the remaining hub cells showed strong TUNEL staining (Fig. 2, D–G). Moreover, 18% of

the testes presented with complete niche loss (Fig. 2 F). Quantification of *hid* by qRT-PCR revealed that the mRNA levels of *hid-3'UTR^{Mut}* were significantly elevated (Fig. 2 H).

Surprisingly, complete removal or replacement of *hid* 3' UTR was even less lethal than *hid-3'UTR^{WT}* (unpublished data), indicating the existence of currently unknown stabilizing elements within the *hid* 3' UTR that oppose the actions of miRNAs and enhance *hid* mRNA stability and/or translation. Next, we used a UAS-*bantam* sponge transgene that contains an artificial 3' UTR region with 20 binding sites for *bantam*, allowing it to quench most *bantam* molecules, making them unavailable to regulate other targets (Herranz et al., 2012). As expected, expression of the *bantam* sponge by itself in the hub did not affect hub viability. However, as depicted in Fig. 2 (I-K) the sponge-induced reduction in *bantam* levels enabled *hid-3'UTR^{WT}* to induce hub cell death. These results provide proof of the principle that the inability of *hid* to induce hub cell death is due at least in part to the action of antiapoptotic *bantam* miRNA.

RNAi-mediated knockdown of *dcr1* in the hub leads to apoptosis

Following the proof of concept that the niche is protected from apoptosis by *bantam*, we tested whether additional miRNAs play a role in protecting the hub of adult males from apoptosis. We therefore disrupted the general process of miRNA production in the hub by RNAi-mediated knockdown of Dcr1, the final processor of all miRNA production. This was done using the TARGET system to drive UAS-*dcr1^{RNAi}* only in the hub of the entire testis. Facilitation of *dcr1* inhibition in this system is possible, since in flies the RNAi and the miRNA pathways use different Dcr enzymes and mutant clones cannot be obtained in postmitotic hub cells (Lee et al., 2004). Immunofluorescence staining of testis from *dcr1^{RNAi}* flies with anti-Dcr1 antibody (Ab) verified that Dcr1 expression is indeed reduced only in the hub cells (Fig. S2, A and B). Because the time window to detect apoptotic events is narrow, we examined testes with TUNEL staining at multiple time points after shifting the conditional *dcr1^{RNAi}* flies to the restrictive temperature (Fig. 3 A). Although many samples showed spontaneous germ cell death (GCD) that occurs often in the germline, no TUNEL signal was observed in the hub of control flies (Fig. 3 B; Yacobi-Sharon et al., 2013). Compared with control, after 6-d incubation of *dcr1^{RNAi}* (*upd-GAL4,GAL80^{ts};UAS-dcr1^{RNAi}*) males at 29°C, the average hub cell number decreased by 30% (Fig. 3, C and G). Nevertheless, all testes contained a functional niche. However, after 8 d, the average hub cell number was reduced by 80% (Fig. 3 G). In these experiments, 70% of the testes showed positive TUNEL staining in hub cells, while the remaining 30% had already lost their niche (Fig. 3 D). Moreover, 100% of testes of *dcr1^{RNAi}* males kept for 14 d at the restrictive temperature presented with a completely absent niche (Fig. 3, E and G). Some of the testes contained remnants of mature sperm, while others had completely empty tubes. Hub cells, CySCs, GSCs, and spermatogonia germ cells were lost, indicating that in the absence of miRNAs, hub cells undergo cell death, causing the neighboring stem cells to detach from the niche and differentiate.

To further confirm that apoptosis is indeed the underlying mechanism for hub death in the absence of miRNAs, we blocked

apoptotic cell death by simultaneous expression of the baculovirus P35 caspase inhibitor (Hay et al., 1995) together with *dcr1^{RNAi}* in the hub (*upd-GAL4;UAS-P35;UAS-dcr1^{RNAi},GAL80^{ts}*). In these experiments, the average hub cell number of the testes of flies raised at 29°C for 16 d increased to four hub cells, and 70% of the testes presented with functional niche (Fig. 3, F and G), indicating that P35 prevented *dcr1^{RNAi}*-induced hub cell loss. To determine that the effect of hub cell death is not caused by off-targets of the *dcr1^{RNAi}* line (24667; Vienna Drosophila Resource Center; VDRC), we tested an additional line (106041; VDRC) that also caused apoptosis of the hub cells. Moreover, RNAi-mediated knockdown of *pasha*, another processor of miRNA biogenesis, also induced hub cell death (Fig. S2, C-G). In contrast with the hub, introduction of *dcr1^{RNAi}* into GSCs, CySCs, and spermatogonia (*esg-GAL4,UAS-gfp;UAS-dcr1^{RNAi},GAL80^{ts}*) did not cause any cell loss (Fig. S2, H and I), which is in agreement with previous findings showing that *dcr1* mutant clones in GSCs exhibit a delayed cell cycle but the cells remain alive (Hatfield et al., 2005). Together, these results indicate that miRNAs have a distinct role in protecting the hub from demise.

Identification of the apoptotic genes that are regulated by miRNA in the hub

We next focused on identifying the specific set of genes that regulate hub apoptosis. For this, we performed a transcriptome analysis of cDNA libraries of four RNA samples each in two biological repeats obtained from testes of conditional *dcr1^{RNAi}* males and age-matched controls at two time points: 6 d, before apoptosis is detected (Fig. 3, C, G, and H), and 8 d, immediately after apoptosis occurs (Fig. 3, D, G, and H). Using differential gene analyses, we focused on changes in genes that are known regulators of apoptosis (Fig. 3 H). Importantly, although *dcr1^{RNAi}* was induced only in hub cells, we were able to detect a significant increase in the levels of nine previously reported apoptosis-associated genes in the 6-d *dcr1^{RNAi}* group, seven of which were also significantly increased in 8-d *dcr1^{RNAi}*. These genes include the transcription factors *grainy head* (*grh*) and *lola* (Cenci and Gould, 2005; Bass et al., 2007), the immune deficiency (*imd*) gene (Georgel et al., 2001), the phagocytic proteins *croquemort* (Franc et al., 1999), and *scab* (Nonaka et al., 2013), and the IAP antagonist *hid* (Fig. 3 H; Grether et al., 1995). In addition to the apoptosis-associated genes, we detected a significant decrease in 13 cell-survival genes in the 8-d *dcr1^{RNAi}*, seven of which were already significantly decreased at 6-d *dcr1^{RNAi}*. These genes include the antiapoptotic factor *DEF related protein 3* (*drep3*; Park and Park, 2012), the telomere maintenance protein *nbs* (Oikemus et al., 2006), and two components of the cell survival EGF pathway, *EGFR* and *Spitz* (Fig. 3 H; Bergmann et al., 1998).

Consistent with these observations, qRT-PCR analysis of RNA extracted from testes of 6- or 8-d conditional *dcr1^{RNAi}* showed a significant enrichment of four apoptosis-associated transcripts (*grh*, *arr1*, *atg7*, and *hid*) relative to age-matched controls (Fig. S3 A). qRT-PCR analysis also verified a significant decrease in two cell survival transcripts (*debcl* and *blm*; Fig. S3 B). Moreover, immunostaining the testis of *dcr1^{RNAi}* with anti-Hid Ab revealed induction of Hid in the hub cells, verifying transcriptome analysis and supporting apoptosis induction of hub cells without miRNAs (Fig. S3, C and D).

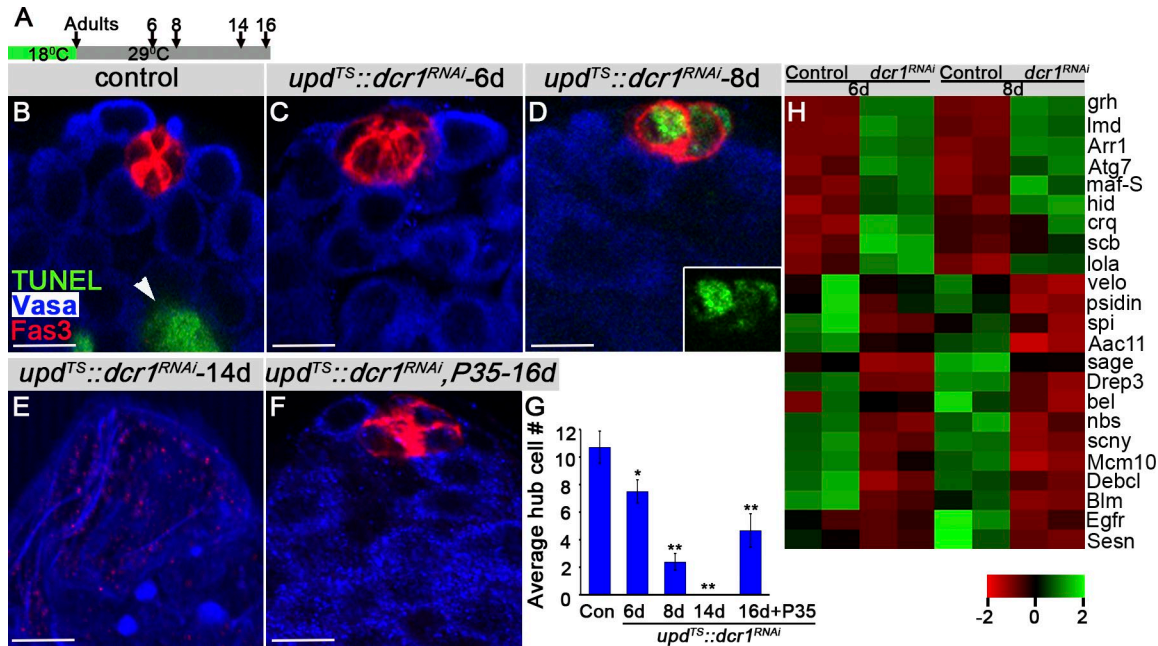


Figure 3. Impaired miRNA biogenesis in the hub leads to regeneration arrest and apoptosis. (A) The scheme for temperature-conditional *dcr1* inactivation in the hub. Flies were developed at the permissive temperature (18°C) and moved to the restrictive temperature (29°C) after eclosion for the amount of days indicated in the image. (B–F) Apical tips of testes immunostained for Fas3 (hub; red), Vasa (blue), and TUNEL (green and inset). (B) Control flies (*upd-GAL4;GAL80^{TS}* outcrossed to *w¹¹¹⁸*), *n* = 35; arrowhead marks spontaneous GCD for TUNEL positive control. (C–E) *upd^{TS}::dcr1^{RNAi}* (*upd-GAL4;UAS-dcr1^{RNAi};GAL80^{TS}*). Apoptosis in the hub (D, 8 d) and niche depletion, and only mature sperms are detected (E, 14 d). (F) P35 rescues *dcr1^{RNAi}* (*upd-GAL4;UAS-P35;UAS-dcr1^{RNAi};GAL80^{TS}*). (G) Shown are average number of hub cells along with 95% confidence intervals (error bars). The total number of testes from *upd::dcr1^{RNAi}* scored: 6 d, *n* = 43; 8 d, *n* = 25; 14 d, *n* = 37; P35 rescues *dcr1^{RNAi}*, *n* = 36. Statistical significance was determined as in Fig. 1 F; *, *P* ≤ 0.05 between 6 d and control; **, *P* ≤ 0.005 between 8 d *dcr1^{RNAi}* and control and P35 rescue. Note that for *dcr1^{RNAi}* at 14 d, the GSC average number is zero. (H) Transcriptome analysis for apoptotic genes whose levels were changed in 6- or 8-d *dcr1^{RNAi}* relative to age-matched controls.

To determine whether induction of proapoptotic genes in *dcr1^{RNAi}* is the main cause for hub cell apoptosis, we reduced both *hid* and *dcr1* simultaneously in the hub for 8 d at 29°C (*upd::UAS-dcr1^{RNAi};UAS-hid^{RNAi}*). These experiments showed that *hid* knockdown completely rescues the *dcr1^{RNAi}* phenotype, indicating that antiapoptosis by miRNAs is a key pathway regulated in the niche to preserve its integrity (Fig. S3, E–H).

Identification of miRNAs that express in the hub

We performed a miRNAome analysis of testes from WT flies using NanoString Fly technology, and ~100 miRNAs were identified and quantified (Table S1). We next hypothesized that the nine apoptosis-associated mRNAs that were found to be elevated before apoptosis in the 6-d *dcr1^{RNAi}* sample are direct targets of miRNAs in the hub. Therefore we used TargetScan Fly bioinformatic prediction software (Ruby et al., 2007) to search for putative miRNA recognition sites in either the 3' UTR or the ORF of these mRNAs (Brodersen and Voinnet, 2009). This search yielded a total of 149 predicted miRNA recognition sites, 32 of which were evolutionarily conserved among closely related species. According to our miRNAome sequencing, 17 of the miRNAs that have predicted conserved recognition sites in the nine apoptosis-associated genes are expressed in the testis (Fig. 4 A and Table S2). As expected, the list included *bantam*, thus supporting library reliability (Brennecke et al., 2003; Ge et al., 2012). The list also included four members of the previously characterized antiapoptotic *miR-2a* family, *miR-13b*, *miR-11*, *miR-2a*, and *miR-13a*, as well

as miRNAs with unknown antiapoptotic function such as *miR-277* (Stark et al., 2003; Esslinger et al., 2013). This analysis revealed that *bantam* and *miR-277* are the two most abundant miRNAs that can each potentially repress four apoptosis-associated mRNA targets (Table S2). To verify whether *bantam* and *miR-277* are indeed expressed in the hub, we used GFP sensors that use the property of miRNAs to silence protein expression. The GFP sensor contains two copies of the complementary sequence for *bantam* or *miR-277* in an artificial 3' UTR region inserted immediately after a reporter GFP sequence (Brennecke et al., 2003). Therefore, if these miRNAs are endogenously expressed in the hub, they create a silencing mechanism that inhibits GFP expression, conferring dark appearance of the hub. Indeed, a comparison between GFP-*bantam* and GFP-*miR-277* and their respective control sensors shows that both are expressed in the hub (Fig. 4, B, C, E, and F). As a negative control, we tested the expression pattern of the GFP-*miR-9a*-sensor (Bejarano et al., 2010) that is not present in the hub and observed a bright GFP signal (Fig. 4 D; Epstein et al., 2017). These data confirm that lack of GFP expression in the hub represents the unique expression pattern of *bantam* and *miR-277*.

miRNAs protect the hub from x-ray and UV irradiation

Removal of miRNAs from the hub by *dcr1^{RNAi}* is a gradual process that ends 14 d after induction at the restrictive temperature and results in niche dissemination (Fig. 3 E). Thus, we postulated that after 6 d (*upd::dcr1^{RNAi}*), the hub becomes sensitized, and the level of many miRNAs is dramatically reduced but not

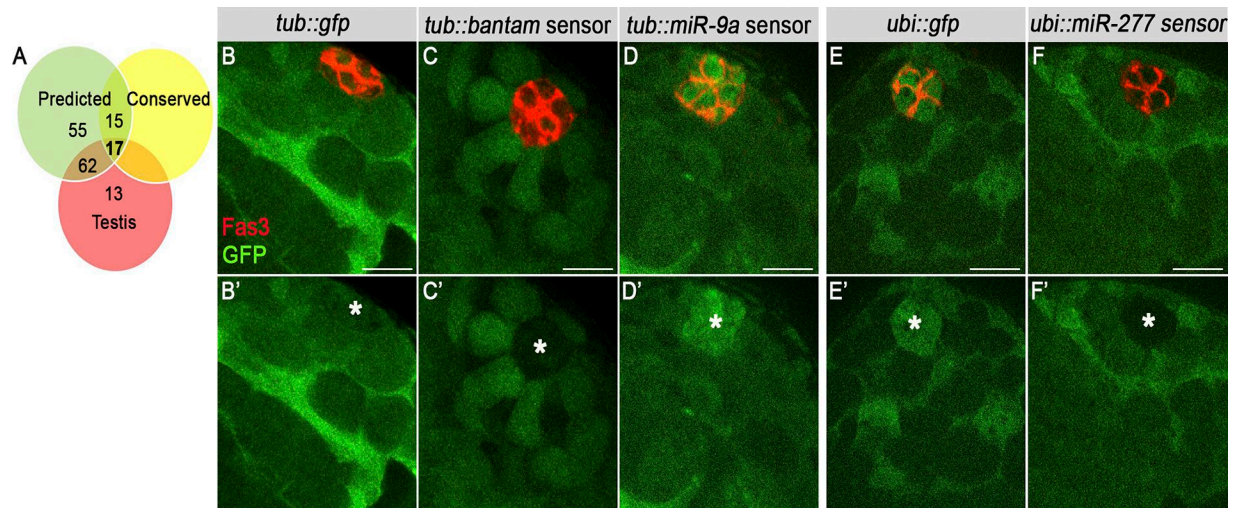


Figure 4. Expression of antiapoptotic miRNAs in the hub. (A) Venn diagram of computationally predicted (green) and evolutionarily conserved miRNAs sites (yellow) for the nine apoptosis-associated genes increased in *dcr1^{RNAi}* compared with the miRNAs that are expressed in the testis according to the NanoString Fly miRNAome (red) revealed 17 potential antiapoptotic miRNAs. (B–F) Testis niches from GFP sensors (green) immunostained for Fas3 (red and asterisks; hub). Testes of control GFP sensor (B and B'), *bantam* sensor (C and C'), and *miR-9a* sensor (D and D') expressed under the Tubulin promoter. Testes of control sensor (E and E') and *miR-277* sensor (F and F') expressed under the Ubiquitin promoter. GFP of control and *miR-9a* sensors (B, D, and E) is expressed in the hub. GFP of *bantam* and *miR-277* sensors is inhibited by endogenous levels of *bantam* and *miR-277* in the hub (C and F).

completely abolished. To find out whether miRNAs in the hub provide protection from external irradiation-induced apoptosis, we irradiated the flies of 6-d conditional *dcr1^{RNAi}* in the hub with x-ray (4,000 rads) or UV (180 kg · m² · s⁻²) radiation. As expected, irradiated control and nonirradiated conditional *dcr1^{RNAi}* showed similar average numbers of hub cells (Fig. 5, A, B, D, and G). However, 100% of the testes examined from irradiated conditional *dcr1^{RNAi}* did not survive apoptosis and showed either TUNEL-positive hub cells (Fig. 5 E) or complete regeneration arrest (Fig. 5 F). This result indicates that the inability of external stress to induce apoptosis can be modulated by a reduction in miRNA levels. In contrast, exposing flies expressing either *bantam* or *miR-277* sponge (*upd-GAL4;UAS-bantam^{SP}* or *upd-GAL4;UAS-miR-277^{SP}*) to the same irradiation protocol was insufficient to induce hub susceptibility to irradiation (not depicted). This suggests that the hub is protected from apoptosis by multiple miRNAs. Because each of the apoptosis-associated genes can be repressed by many miRNAs (e.g., *hid* 3' UTR may be potentially regulated by >20 miRNAs), knocking down one miRNA is insufficient to affect hub resistance to irradiation.

Moreover, our transcriptome and qRT-PCR analyses showed that without miRNAs in the hub, the transcript levels of the transcription factor *grh* increases by 12-fold. We therefore hypothesized that overexpression of the Grh coding region, which lacks most of the 3' UTR, and miRNA recognition sites (including 89/1,946 bp; Baumgardt et al., 2009), should also result in a sensitized hub for irradiation. As shown in Fig. 5 I, Grh overexpression indeed sensitized the hub to UV irradiation (180 kg · m² · s⁻²), and 58% of the testes showed strong TUNEL staining. These data suggest that under normal conditions, the expression of *grh* is repressed by miRNAs to prevent hub loss.

In summary, knockdown of miRNAs in the hub resulted in the induction of several apoptosis-associated genes including transcription factors and the IAP antagonist *hid*, indicating that

miRNAs are incorporated into a large regulatory network that prevents hub apoptosis. The expression of the IAP antagonists *rpr*, *hid*, and *grim* is tightly repressed in living cells. However, they are rapidly up-regulated in response to an apoptotic signal and induce cell death by competitively binding and antagonizing Diap1, which leads to activation of the cell death program (Vasudevan and Ryoo, 2015). Antiapoptotic miRNAs that inhibit IAP antagonist translation act at the level of execution, which is practically downstream of all apoptotic events. In this study, we show that overexpression of IAP antagonists, which induces apoptosis in many cell types (Grether et al., 1995; Chen et al., 1996; White et al., 1996; Hétié et al., 2014), is unable to kill the hub cells. This implies that the hub contains a strong antiapoptotic mechanism. In contrast, removal of miRNA expression from the hub is in itself sufficient to induce hub cell death and as such may serve as a future strategy to induce death in tumors that are resistant to apoptosis by genotoxic signals.

The function of the hub is to keep the stem cells in an undifferentiated state, and spermatogenesis can be maintained even when only one hub cell remains alive (Resende et al., 2013). However, when all hub cells die, spermatogenesis cannot be regained and the testis degenerates. We show that several miRNAs that are expressed in the hub protect it from apoptosis. Nevertheless, knocking down one miRNA is insufficient to affect hub resistance to irradiation. These results are in line with previous findings, indicating that individual miRNAs are not essential for viability (Miska et al., 2007). Nonetheless, because the hub is resistant to a variety of harmful signals, additional protective mechanisms besides miRNAs are probably involved in preservation of hub integrity.

Contrary to other regenerative tissues where antiapoptotic miRNAs are found primarily in the stem cells themselves (Hatfield et al., 2005; Weng and Cohen, 2015; Xing et al., 2015), we found that in the *Drosophila* testis, they are expressed in

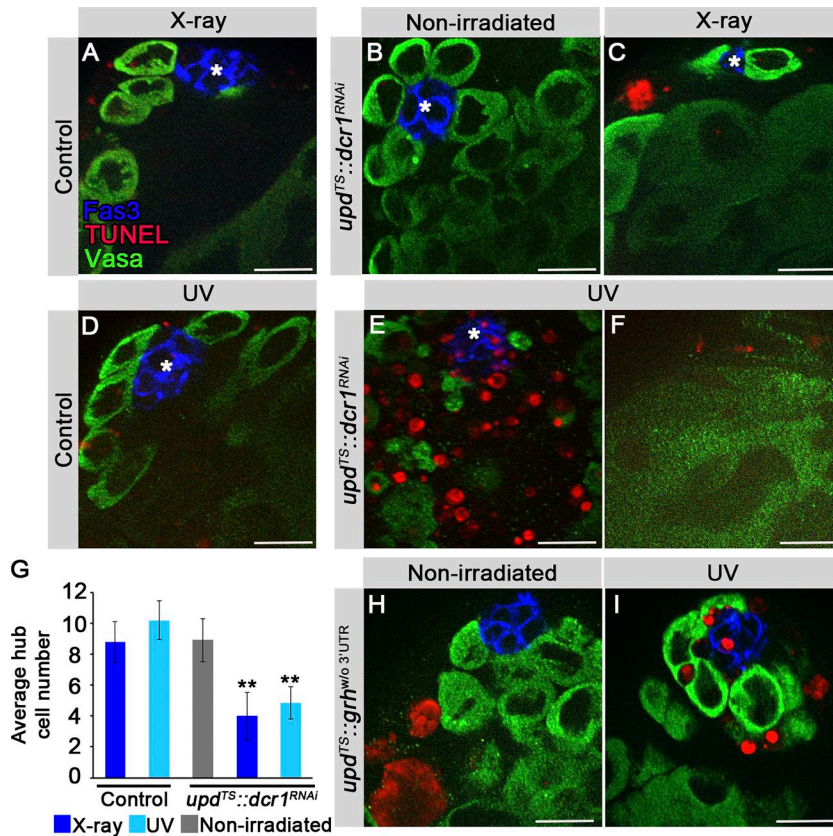


Figure 5. miRNAs protect the hub from irradiation-induced apoptosis. (A–F) Testes of flies raised for 6 d at 29°C immunostained for Fas3 (hub; blue and asterisk), TUNEL (red), and Vasa (germ cells; green). Control flies (*upd-GAL4,GAL80^{TS}* outcrossed to *w¹¹¹⁸*) irradiated with x-ray (A; 4,000 rad) or UV (D; 180 kg · m² · s⁻²). *dcr1^{RNAi}* flies (*upd-GAL4;UAS-dcr1^{RNAi},GAL80^{TS}*), nonirradiated (B) or x-ray (C) or UV; two examples of representative testis: TUNEL in the hub (E) or complete disappearance of the hub resulting in regeneration arrest (F). **(G)** Shown are average hub cell number per testis along with 95% confidence intervals (error bars) in control and *dcr1^{RNAi}* flies after UV and x-ray irradiation. The total number of testes from 6 d *upd::dcr1^{RNAi}* scored: *n* = 25 nonirradiated, *n* = 23 UV-irradiated, and *n* = 22 x-ray-irradiated. Controls: UV-irradiated, *n* = 27; x-ray-irradiated, *n* = 21. Statistical significance was determined as in Fig. 1 F; **, *P* ≤ 0.005 between *dcr1^{RNAi}* irradiated (UV and x-ray) and nonirradiated or irradiated control. **(H and I)** Overexpression of Grh without 3' UTR in the hub (*upd^{TS}::grh^{w/o} 3'UTR*) resulted in minor apoptosis in the hub (H; 2/33) but induced sensitivity to hub cell death after UV irradiation in 58% of the testes examined (I; TUNEL in the hub, 26/44).

the postmitotic niche cells. We propose that because male spermatogonia germ cells have the unique ability to dedifferentiate and regain GSC identity (Brawley and Matunis, 2004), an antiapoptotic propensity in them is dispensable. Rather, the ability to protect the reproductive system from apoptosis must be maintained by the postmitotic niche cells that nonautonomously enable recovery of the stem cell population after irradiation.

Materials and methods

Generation of DNA constructs

pUASTattB-*hid FL*, pUASTattB-*hid-3'UTR^{Mut}*, pUASTattB-*rpr*, and pUASTattB-*grim* were generated in our laboratory by cloning the genes with their 3' UTR into pUASTattB plasmid. *hid* CR was amplified by PCR from pUAST-*hidMF* plasmid (a gift from H. Steller) with forward primer Hid_CR_For, 5'-ATGGCCGTGCCCTTTTATTGCGGAGGCGGCGCCG-3', and reverse primer Hid_CR_HA_Rev2, 5'-TCAAGCGTAGTCTGGGACGTGATGGGTATCGCGCCGCAAAGAAGCCACAGCCC-3'. The PCR fragment was ligated into pGEM T Easy vector, and the insert was further digested with EcoR1 and cloned into EcoR1, digested, and calf intestinal alkaline phosphatase (CIP) treated with pUASTattB to generate pUASTattB *hid* CR. *hid* 3' UTR was amplified by PCR from pUAST-*hidMF* plasmid (a gift from H. Steller) with forward primer Hid3'UTR_For, 5'-GGACTAGtAAGCGCAGGAGACGTGTAATCG-3', and reverse primer Hid3'UTR_Rev, 5'-GGACTAGTGGCCTTTTATTTCATTTACACATAC-3'. PCR fragment was ligated into pJET1.2 vector, and the insert was further digested with BglII and cloned into BglII, digested, and CIP treated with pUASTattB *hid* CR

to generate pUASTattB *hid FL*. To generate pUASTattB-*hid-3'UTR^{Mut}*, site-directed mutagenesis (Stratagene) was used to mutate two *bantam* recognition sites in *hid-3' UTR* (¹⁰⁴¹ATC = GCA and ¹²³³ATC = GCA) with primers Bantam2_mut_For, 5'-TGGAAATTAATGAAAATGGCATCCGCAGCTAGCC-3', Bantam2_mut_Rev, 5'-GGCTAGCTGCGGATGCCAATTTTCATTAATTTCCA-3', Bantam3_mut_For, 5'-CCAATTCCCAAAAATCGCATTGGCATCATGGATTATAC-3', and Bantam3_mut_Rev, 5'-GTATAAATCCATGATGCCAATGCGATTTTGGGAATTGG-3'.

grim with its 3' UTR was amplified by PCR from pUAST-*grimMF* plasmid (a gift from H. Steller) with forward primer Grim_CR_For, 5'-ATGGCCATCGCCTATTTGATACCCG-3', and reverse primer Grim_3'UTR_Rev, 5'-GGACTAGTGTTATTTTTCCTTGTGTC-3'. Similarly, *rpr* with its 3' UTR was amplified by PCR from *reaper-HA3-PUAST* plasmid (a gift from H. Steller) with forward primer Rpr5_For, 5'-TCATTGAATAAGAGAGACACCAGAA-3', and reverse primer Rpr_3'UTR_Rev, 5'-CCCAAGCTTTTCGACTCATCTTCG-3'.

PCR fragments of *grim* and *rpr* were ligated into pGEM T Easy vector, and the inserts were further digested with EcoR1 and cloned into EcoR1, digested, and CIP treated with pUASTattB to generate pUASTattB-*grim* and pUASTattB-*rpr*, respectively. The sequence of all DNA constructs described above was verified by DNA sequencing.

Drosophila stocks

Flies were raised at 25°C on standard cornmeal molasses agar medium freshly prepared in our laboratory. Crosses for the inducible GAL4/UAS TARGET system (McGuire et al., 2004)

were set up and maintained at 18°C until eclosion. Adults were placed in vials (20 males and 20 females per vial), kept at 29°C, and flipped every 2 d thereafter. Control and experiments were set and tested at the same time. Fly strains used in this research were *w¹¹¹⁸*, control Tub-GFP sensor, Tub-*bantam*-GFP sensor, Tub-*hid*-3'UTR reporter, Tub-*grim*-3'UTR reporter (S.M. Cohen; Brennecke et al., 2003), Tub-*miR-9a*-GFP sensor (E.C. Lai; Bejarano et al., 2010), control Ubi-GFP sensor, Ubi-*miR-277*-GFP sensor (K. Förstemann; Esslinger et al., 2013), *upd-GAL4* (T. Xie), *upd-GAL4;GAL80^{TS}* (D.L. Jones) *UAS-dcr1^{RNAi}* lines (24667 and 4106041; VDRC), and *UAS-pasha^{RNAi}* and *UAS-hid^{RNAi}* (40118 and 8269; VDRC). To simultaneously knockdown *hid* and *dcr1*, we generated a recombinant line on the third chromosome (Rec#1, *UAS-hid^{RNAi}*, *UAS-dcr1^{RNAi}*) PUAAS-grh.B12M (Bloomington Drosophila Stock Center; Baumgardt et al., 2009). The *esg-GAL4,UAS-gfp;GAL80ts* was made from *esg-GAL4,UAS-gfp*, and *GAL80ts* (Loza-Coll et al., 2014). pUASTattB-*hid FL*, pUASTattB-*hid*-3'UTR^{Mut}, pUASTattB-*rpr*, and pUASTattB-*grim* were injected into *y,w*; attP2 (third chromosome; 8622; Bloomington Drosophila Stock Center) with BestGene.

Immunofluorescence TUNEL and stem cell counting

Wholemout testes from adult *Drosophila* were dissected in PBS and placed in Terasaki plates in 10 µl fixed solution of 2% PFA in PLP buffer (0.075 M lysine and 0.01 M sodium phosphate buffer, pH 7.4) for 1 h at RT, rinsed, and washed twice in PBST (0.5% Triton X-100), followed by standard immunofluorescence staining. Primary antibodies used in this study were as follows: polyclonal rabbit anti-Vasa (1:200; d-260; Santa Cruz Biotechnology), rabbit anti-Dcr1 (1:100; PA5-19429; Thermo Fisher Scientific), rabbit anti-Hid (1:50; d-300; Santa Cruz Biotechnology), and mouse anti-Fas3 (1:10; 7G10; Developmental Studies Hybridoma Bank). Secondary antibodies were obtained from Jackson ImmunoResearch Laboratories. For TUNEL labeling, testes were refixed, washed, and labeled with the In Situ Cell Death Detection kit (Roche) according to the manufacturer's instructions. Samples were mounted in Vectashield mounting medium with DAPI (Vector Laboratories).

Microscope image acquisition

Images were taken from samples at RT on a Zeiss AxioImager M2 microscope equipped with an ApoTome2 Optical sectioning device. The image shown in Fig. S1 A was taken with objective Plan Apochromat 20×/0.8 M27; all the other images in the manuscript were taken with objective Plan Apochromat 63×/1.40 oil M27. All images in all figures are single sections that were taken with high-resolution microscopy camera AxioCam HRm Rev.3 FireWire using Zen acquisition software and were processed with Adobe Photoshop CS6. GSCs were counted from multiple z stacks as Vasa-positive cells that were in direct contact with the hub that was marked with anti-Fas3.

X-ray irradiation

WT (*w¹¹¹⁸*) or *upd::dcr1^{RNAi}* that were maintained for 6 d at 29°C were irradiated with 4,000 rads, and then recovered for 4 or 24 h or 17 d at 25°C. After recovery, testes were dissected and subjected to immunofluorescence and TUNEL labeling.

RNA extraction

Testes of 100 flies (~200 testes) of each phenotype and age were dissected in PBS diethyl pyrocarbonate. Testes were collected and pooled in 100 µl TRIZOL reagent and stored at -80°C until RNA extraction. To maximize RNA extraction, frozen samples were thawed at 37°C and refrozen in liquid nitrogen (-80°C) five times followed by five cycles of 30-s vortex and rest. Then, 100 µl of 99% ethanol was added to the samples, and total RNA was extracted using Direct-zol RNA miniprep kit (Zymo Research) with DNase treatment according to the manufacturer's instructions. The RNA was eluted in 50 µl preheated DNase- and RNase-free water and kept at -80°C for future use. RNA quality was measured by a BioAnalyzer, and samples were used for miRNAome, transcriptome, or qRT-PCR.

Transcriptome analysis and statistics

Illumina cDNA libraries were prepared with TruSeq RNA V2/Illumina kit from 1 µg total RNA extracted from testes of four RNA samples each in two biological repeats. The four samples were conditional *dcr1^{RNAi}* males (*upd-GAL4,GAL80^{ts};UAS-dcr1^{RNAi}*) and age-matched controls (*upd-GAL4,GAL80^{ts}* outcrossed to *w¹¹¹⁸*) that were raised at 29°C for 6 and 8 d. Libraries were prepared and sequenced with Illumina HiSeq 2500 at the Technion Genome Center. Raw reads were filtered for Illumina adapters, and low-quality reads, using Trimmomatic. Filtered reads were aligned to the *Drosophila* genome (dm6, FlyBase 6.05) using STAR (settings: alignIntronMax = 25,000; genomeSAindexNbases = 9.15; sjdbGTFfile). Gene expression levels were quantified using htseq-count, and differential expression was analyzed using edgeR. Differential expression data were filtered based on fold change (1.3 < FC < -1.3) and significance cutoff ($P \leq 0.05$). We then searched the list for apoptotic genes that showed differential expression in conditional *dcr1^{RNAi}* males versus control in both testes from 6 and 8 d.

miRNAome analysis and statistics

Total purified RNA samples (0.5 µg at 100 ng/µl) of WT *w¹¹¹⁸* in three biological repeats were used to determine the identity and levels of miRNAs with NanoString Technologies (nCounter fly miRNA expression kit). Raw data were normalized using nCounter software and compared with a list of *in silico* predicted miRNAs for the nine apoptosis-associated genes (TargetScan Fly; Ruby et al., 2007).

qRT-PCR and statistics

1 µg RNA was reverse transcribed with random hexamer mixture and the High-Capacity cDNA Reverse Transcription Kit (Thermo Fisher Scientific) according to manufacturer's instructions. Quantitative real-time PCR was performed with a StepOnePlus Real-time PCR System using TaqMan Gene Expression Assay (Applied Biosystems). Relative *hid* (assay ID: Dm01823031_m1) levels were compared with Ribosomal Protein L32 (RPL-32; assay ID: Dm02151827_g1). For other genes, we used SYBR Green PCR Master mix (Applied Biosystems), and the efficiency of the target and reference amplification was approximately equal. Specific primers for qRT-PCR of testes were *grh* forward, 5'-CGAGGAAGT GTCGCACAA-3', and reverse, 5'-GAACCGCAATGTTGATCTTG-3';

arr1 forward, 5'-AGCTACCATTATTCTGATGCAC-3', and reverse, 5'-GGTAGCCCTTTTCAGTTTAGGC-3'; *atg7* forward, 5'-TAAGGAAGCAGGCGACGA-3', and reverse, 5'-CCAAAGTTGGTCTTTGAGC-3'; *hid* forward, 5'-CCTCTACGAGTGGGTCAGGA-3', and reverse, 5'-GCGGATACTGGAAGATTTGC-3'; *debl* forward, 5'-AGT TTTCCGGGACTGAAC-3', and reverse, 5'-GCTGTGCGGATATGT TTGTG-3'; and *blm* forward, 5'-AATCAATAAACTGGCTTCCCT AGA-3', and reverse, 5'-TCACGTAGAGCAATTTGACCA-3'. Levels were compared with the average of two normalizing genes: *act24A* forward, 5'-TCTTACTGAGCGGGTTACAG-3', and reverse, 5'-ATGTCGCGCACAATTTAC-3'; and *sdhA* forward, 5'-CGTGTG CCATCGATTTT-3', and reverse, 5'-CTTCGATATCTGTCCGG ATTC-3'. Real-time PCR results were analyzed using StepOne software (Applied Biosystems), and significance was determined using Student's *t* test. An average of three experiments (each performed in triplicate measurements) is shown (mean \pm SD).

Statistical analysis

For quantification of GSCs and hub cell number, the mean \pm 95% confidence interval and the number (*n*) of testes examined are shown. *P* values were generated after a two-tailed Student's *t* test or determined by one-way ANOVA, and post hoc analysis was performed with Tukey multicomparison test if samples were normally distributed and had equal variances: *, *P* \leq 0.01; **, *P* \leq 0.005. The Shapiro–Wilk test, which is appropriate for small sample sizes (<50 samples), was used with SPSS software to determine normality.

Online supplemental material

Fig. S1 shows that *upd^{TS}* drives expression only in the hub cells of the entire testis. Fig. S2 illustrates that impaired miRNA biogenesis in the hub leads to apoptosis but does not affect the viability of germ and cyst cells. Fig. S3 provides verification for the transcriptome analysis. Table S1 presents the miRNAs that are expressed in the *Drosophila* testis, and Table S2 shows the potential antiapoptotic miRNAs that are expressed in the hub cells.

Acknowledgments

We are grateful to Herman Steller (Rockefeller University, New York, NY), Stephen M. Cohen (University of Copenhagen, Copenhagen, Denmark), Eric C. Lai (Sloan-Kettering Memorial Institute, New York, NY), Adi Salzberg (Technion-Israel Institute of Technology, Haifa, Israel), D. Leanne Jones (University of California, Los Angeles, Los Angeles, CA), Eli Arama, Keren Yacobi-Sharon, Ben-Zion Shilo, Shari Carmon (Weizmann Institute of Science, Rehovot, Israel), Rohit Joshi (Centre for DNA Fingerprinting and Diagnostics, Hyderabad, India), Bih-Hwa Shieh (Vanderbilt University, Nashville, TN), Neal Silverman (University of Massachusetts Medical School, Worcester, MA), Stefan Thor (Linköping University, Linköping, Sweden), and the Developmental Studies Hybridoma Bank for gracious gifts of *Drosophila* stocks, plasmids, and antibodies that were critical for this study. We also thank Liza Barki-Harrington and Doron Chelouche for advice and comments and Alex Nevelsky for the assistance in the x-ray experiments.

This work was supported by the Israel Science Foundation personal grant to H. Toledano (1510/14).

The authors declare no competing financial interests.

Author contributions: M. Volin, M. Zohar-Fux, and O. Gonen designed and performed the in vivo experiments. M. Volin and L. Porat-Kuperstein performed the qRT-PCR and transcriptome analysis. M. Volin and O. Gonen performed the miRNAome analysis. H. Toledano designed the study, coordinated the project, and wrote the manuscript with input from all authors.

Submitted: 16 November 2017

Revised: 10 December 2017

Accepted: 25 July 2018

References

- Arama, E., and H. Steller. 2006. Detection of apoptosis by terminal deoxynucleotidyl transferase-mediated dUTP nick-end labeling and acridine orange in *Drosophila* embryos and adult male gonads. *Nat. Protoc.* 1:1725–1731. <https://doi.org/10.1038/nprot.2006.235>
- Bass, B.P., K. Cullen, and K. McCall. 2007. The axon guidance gene *lola* is required for programmed cell death in the *Drosophila* ovary. *Dev. Biol.* 304:771–785. <https://doi.org/10.1016/j.ydbio.2007.01.029>
- Baumgardt, M., D. Karlsson, J. Terriente, F.J. Diaz-Benjumea, and S. Thor. 2009. Neuronal subtype specification within a lineage by opposing temporal feed-forward loops. *Cell.* 139:969–982. <https://doi.org/10.1016/j.cell.2009.10.032>
- Bejarano, F., P. Smibert, and E.C. Lai. 2010. miR-9a prevents apoptosis during wing development by repressing *Drosophila* LIM-only. *Dev. Biol.* 338:63–73. <https://doi.org/10.1016/j.ydbio.2009.11.025>
- Bergmann, A., J. Agapite, K. McCall, and H. Steller. 1998. The *Drosophila* gene *hid* is a direct molecular target of Ras-dependent survival signaling. *Cell.* 95:331–341. [https://doi.org/10.1016/S0092-8674\(00\)81765-1](https://doi.org/10.1016/S0092-8674(00)81765-1)
- Brawley, C., and E. Matunis. 2004. Regeneration of male germline stem cells by spermatogonial dedifferentiation in vivo. *Science.* 304:1331–1334. <https://doi.org/10.1126/science.1097676>
- Bree, R.T., C. Stenson-Cox, M. Grealy, L. Byrnes, A.M. Gorman, and A. Samali. 2002. Cellular longevity: role of apoptosis and replicative senescence. *Biogerontology.* 3:195–206. <https://doi.org/10.1023/A:1016299812327>
- Brennecke, J., D.R. Hipfner, A. Stark, R.B. Russell, and S.M. Cohen. 2003. Bantam encodes a developmentally regulated microRNA that controls cell proliferation and regulates the proapoptotic gene *hid* in *Drosophila*. *Cell.* 113:25–36. [https://doi.org/10.1016/S0092-8674\(03\)00231-9](https://doi.org/10.1016/S0092-8674(03)00231-9)
- Brodersen, P., and O. Voinnet. 2009. Revisiting the principles of microRNA target recognition and mode of action. *Nat. Rev. Mol. Cell Biol.* 10:141–148. <https://doi.org/10.1038/nrm2619>
- Cenci, C., and A.P. Gould. 2005. *Drosophila* Grainyhead specifies late programmes of neural proliferation by regulating the mitotic activity and Hox-dependent apoptosis of neuroblasts. *Development.* 132:3835–3845. <https://doi.org/10.1242/dev.01932>
- Chen, P., W. Nordstrom, B. Gish, and J.M. Abrams. 1996. Grim, a novel cell death gene in *Drosophila*. *Genes Dev.* 10:1773–1782. <https://doi.org/10.1101/gad.10.14.1773>
- Djuranovic, S., A. Nahvi, and R. Green. 2012. miRNA-mediated gene silencing by translational repression followed by mRNA deadenylation and decay. *Science.* 336:237–240. <https://doi.org/10.1126/science.1215691>
- Epstein, Y., N. Perry, M. Volin, M. Zohar-Fux, R. Braun, L. Porat-Kuperstein, and H. Toledano. 2017. miR-9a modulates maintenance and ageing of *Drosophila* germline stem cells by limiting N-cadherin expression. *Nat. Commun.* 8:600. <https://doi.org/10.1038/s41467-017-00485-9>
- Esslinger, S.M., B. Schwalb, S. Helfer, K.M. Michalik, H. Witte, K.C. Maier, D. Martin, B. Michalke, A. Tresch, P. Cramer, and K. Förstemann. 2013. *Drosophila* miR-277 controls branched-chain amino acid catabolism and affects lifespan. *RNA Biol.* 10:1042–1056. <https://doi.org/10.4161/rna.24810>
- Franc, N.C., P. Heitzler, R.A. Ezekowitz, and K. White. 1999. Requirement for croquemort in phagocytosis of apoptotic cells in *Drosophila*. *Science.* 284:1991–1994. <https://doi.org/10.1126/science.284.5422.1991>
- Ge, W., Y.W. Chen, R. Weng, S.F. Lim, M. Buescher, R. Zhang, and S.M. Cohen. 2012. Overlapping functions of microRNAs in control of apoptosis during *Drosophila* embryogenesis. *Cell Death Differ.* 19:839–846. <https://doi.org/10.1038/cdd.2011.161>

- Georgel, P., S. Naitza, C. Kappler, D. Ferrandon, D. Zachary, C. Swimmer, C. Kopczyński, G. Duyk, J.M. Reichhart, and J.A. Hoffmann. 2001. Drosophila immune deficiency (IMD) is a death domain protein that activates antibacterial defense and can promote apoptosis. *Dev. Cell.* 1:503–514. [https://doi.org/10.1016/S1534-5807\(01\)00059-4](https://doi.org/10.1016/S1534-5807(01)00059-4)
- Ghildiyal, M., and P.D. Zamore. 2009. Small silencing RNAs: an expanding universe. *Nat. Rev. Genet.* 10:94–108. <https://doi.org/10.1038/nrg2504>
- Grether, M.E., J.M. Abrams, J. Agapite, K. White, and H. Steller. 1995. The head involution defective gene of *Drosophila melanogaster* functions in programmed cell death. *Genes Dev.* 9:1694–1708. <https://doi.org/10.1101/gad.9.14.1694>
- Hatfield, S.D., H.R. Shcherbata, K.A. Fischer, K. Nakahara, R.W. Carthew, and H. Ruohola-Baker. 2005. Stem cell division is regulated by the microRNA pathway. *Nature.* 435:974–978. <https://doi.org/10.1038/nature03816>
- Hay, B.A., D.A. Wassarman, and G.M. Rubin. 1995. Drosophila homologs of baculovirus inhibitor of apoptosis proteins function to block cell death. *Cell.* 83:1253–1262. [https://doi.org/10.1016/0092-8674\(95\)90150-7](https://doi.org/10.1016/0092-8674(95)90150-7)
- Herranz, H., X. Hong, and S.M. Cohen. 2012. Mutual repression by bantam miRNA and Capicua links the EGFR/MAPK and Hippo pathways in growth control. *Curr. Biol.* 22:651–657. <https://doi.org/10.1016/j.cub.2012.02.050>
- Hétie, P., M. de Cuevas, and E. Matunis. 2014. Conversion of quiescent niche cells to somatic stem cells causes ectopic niche formation in the *Drosophila* testis. *Cell Reports.* 7:715–721. <https://doi.org/10.1016/j.celrep.2014.03.058>
- Insko, M.L., A. Leon, C.H. Tam, D.M. McKearin, and M.T. Fuller. 2009. Accumulation of a differentiation regulator specifies transit amplifying division number in an adult stem cell lineage. *Proc. Natl. Acad. Sci. USA.* 106:22311–22316. <https://doi.org/10.1073/pnas.0912454106>
- Jones, D.L., and A.J. Wagers. 2008. No place like home: anatomy and function of the stem cell niche. *Nat. Rev. Mol. Cell Biol.* 9:11–21. <https://doi.org/10.1038/nrm2319>
- Kiger, A.A., D.L. Jones, C. Schulz, M.B. Rogers, and M.T. Fuller. 2001. Stem cell self-renewal specified by JAK-STAT activation in response to a support cell cue. *Science.* 294:2542–2545. <https://doi.org/10.1126/science.1066707>
- Leatherman, J.L., and S. Dinardo. 2010. Germline self-renewal requires cyst stem cells and stat regulates niche adhesion in *Drosophila* testes. *Nat. Cell Biol.* 12:806–811. <https://doi.org/10.1038/ncb2086>
- Lee, Y.S., K. Nakahara, J.W. Pham, K. Kim, Z. He, E.J. Sontheimer, and R.W. Carthew. 2004. Distinct roles for *Drosophila* Dicer-1 and Dicer-2 in the siRNA/miRNA silencing pathways. *Cell.* 117:69–81. [https://doi.org/10.1016/S0092-8674\(04\)00261-2](https://doi.org/10.1016/S0092-8674(04)00261-2)
- Lin, H. 2002. The stem-cell niche theory: lessons from flies. *Nat. Rev. Genet.* 3:931–940. <https://doi.org/10.1038/nrg952>
- Loza-Coll, M.A., T.D. Southall, S.L. Sandall, A.H. Brand, and D.L. Jones. 2014. Regulation of *Drosophila* intestinal stem cell maintenance and differentiation by the transcription factor Escargot. *EMBO J.* 33:2983–2996. <https://doi.org/10.15252/embj.201489050>
- McGuire, S.E., Z. Mao, and R.L. Davis. 2004. Spatiotemporal gene expression targeting with the TARGET and gene-switch systems in *Drosophila*. *Sci. STKE.* 2004:pl6.
- Miska, E.A., E. Alvarez-Saavedra, A.L. Abbott, N.C. Lau, A.B. Hellman, S.M. McGonagle, D.P. Bartel, V.R. Ambros, and H.R. Horvitz. 2007. Most *Caenorhabditis elegans* microRNAs are individually not essential for development or viability. *PLoS Genet.* 3:e215. <https://doi.org/10.1371/journal.pgen.0030215>
- Morrison, S.J., and A.C. Spradling. 2008. Stem cells and niches: mechanisms that promote stem cell maintenance throughout life. *Cell.* 132:598–611. <https://doi.org/10.1016/j.cell.2008.01.038>
- Nonaka, S., K. Nagaosa, T. Mori, A. Shiratsuchi, and Y. Nakanishi. 2013. Integrin α PS3/ β v-mediated phagocytosis of apoptotic cells and bacteria in *Drosophila*. *J. Biol. Chem.* 288:10374–10380. <https://doi.org/10.1074/jbc.M113.451427>
- Oikemus, S.R., J. Queiroz-Machado, K. Lai, N. McGinnis, C. Sunkel, and M.H. Brodsky. 2006. Epigenetic telomere protection by *Drosophila* DNA damage response pathways. *PLoS Genet.* 2:e71. <https://doi.org/10.1371/journal.pgen.0020071>
- Park, O.K., and H.H. Park. 2012. Dual apoptotic DNA fragmentation system in the fly: Drep2 is a novel nuclease of which activity is inhibited by Drep3. *FEBS Lett.* 586:3085–3089. <https://doi.org/10.1016/j.febslet.2012.07.056>
- Resende, L.P., M. Boyle, D. Tran, T. Fellner, and D.L. Jones. 2013. Headcase promotes cell survival and niche maintenance in the *Drosophila* testis. *PLoS One.* 8:e68026. <https://doi.org/10.1371/journal.pone.0068026>
- Ruby, J.G., A. Stark, W.K. Johnston, M. Kellis, D.P. Bartel, and E.C. Lai. 2007. Evolution, biogenesis, expression, and target predictions of a substantially expanded set of *Drosophila* microRNAs. *Genome Res.* 17:1850–1864. <https://doi.org/10.1101/gr.6597907>
- Saxe, J.P., and H. Lin. 2011. Small noncoding RNAs in the germline. *Cold Spring Harb. Perspect. Biol.* 3:a002717. <https://doi.org/10.1101/cshperspect.a002717>
- Stark, A., J. Brennecke, R.B. Russell, and S.M. Cohen. 2003. Identification of *Drosophila* microRNA targets. *PLoS Biol.* 1:E60. <https://doi.org/10.1371/journal.pbio.0000060>
- Steller, H. 2008. Regulation of apoptosis in *Drosophila*. *Cell Death Differ.* 15:1132–1138. <https://doi.org/10.1038/cdd.2008.50>
- Tulina, N., and E. Matunis. 2001. Control of stem cell self-renewal in *Drosophila* spermatogenesis by JAK-STAT signaling. *Science.* 294:2546–2549. <https://doi.org/10.1126/science.1066700>
- Vasudevan, D., and H.D. Ryo. 2015. Regulation of cell death by IAPs and their antagonists. *Curr. Top. Dev. Biol.* 114:185–208. <https://doi.org/10.1016/bs.ctdb.2015.07.026>
- Weng, R., and S.M. Cohen. 2015. Control of *Drosophila* Type I and Type II central brain neuroblast proliferation by bantam microRNA. *Development.* 142:3713–3720. <https://doi.org/10.1242/dev.127209>
- White, K., E. Tahaoglu, and H. Steller. 1996. Cell killing by the *Drosophila* gene reaper. *Science.* 271:805–807. <https://doi.org/10.1126/science.271.5250.805>
- Xing, Y., T.T. Su, and H. Ruohola-Baker. 2015. Tie-mediated signal from apoptotic cells protects stem cells in *Drosophila melanogaster*. *Nat. Commun.* 6:7058. <https://doi.org/10.1038/ncomms8058>
- Xu, D., S.E. Woodfield, T.V. Lee, Y. Fan, C. Antonio, and A. Bergmann. 2009. Genetic control of programmed cell death (apoptosis) in *Drosophila*. *Fly (Austin).* 3:78–90. <https://doi.org/10.4161/fly.3.1.7800>
- Yacobi-Sharon, K., Y. Namdar, and E. Arama. 2013. Alternative germ cell death pathway in *Drosophila* involves HtrA2/Omi, lysosomes, and a caspase-9 counterpart. *Dev. Cell.* 25:29–42. <https://doi.org/10.1016/j.devcel.2013.02.002>